

## Local spin-density electronic structures and magnetic properties of small iron clusters

This article has been downloaded from IOPscience. Please scroll down to see the full text article.

1995 J. Phys.: Condens. Matter 7 2421

(<http://iopscience.iop.org/0953-8984/7/12/006>)

View [the table of contents for this issue](#), or go to the [journal homepage](#) for more

Download details:

IP Address: 171.66.16.179

The article was downloaded on 13/05/2010 at 12:48

Please note that [terms and conditions apply](#).

## Local spin-density electronic structures and magnetic properties of small iron clusters

X G Gong and Q Q Zheng

Centre for Theoretical Physics, Chinese Centre of Advanced Science and Technology (World Laboratory), Box 8730, Beijing and Institute of Solid State Physics, Academia Sinica, 230031-Hefei, People's Republic of China

Received 29 September 1994, in final form 28 November 1994

**Abstract.** The atomic structures and physical properties of small iron clusters have been calculated using density functional theory with the local spin-density approximation. We have found that the small iron clusters tend to form compact structures. The magnetic moments are found to be larger than the bulk value, which is in good agreement with experimental data. The results on the electronic properties and ionization potentials for small clusters in the ground state are also discussed.

Atomic clusters constitute an intermediate phase between atom and bulk phases, which shows anomalous physical and chemical properties in comparison with the behaviour of the corresponding bulk solids and free atoms. In recent years, much effort has been made theoretically and experimentally to understand the physics of clusters. Transition-metal clusters are of particular interest, because their significant catalytic and magnetic properties have led to useful technological applications, such as in high-density magnetic devices [1]. The experimental results on magnetic properties and electronic structures of transition-metal clusters have stimulated extensive theoretical investigations. Cox *et al* [2] and de Heer *et al* [3] have reported the results of Stern–Gerlach deflection experiments with iron clusters, where they found the magnetization increasing with the applied field. As we know, the magnetism of atoms is localized, while the magnetism of bulk phases is largely dependent on the d-band filling, lattice structure, and so on. The measured magnetic moments for the iron clusters reported recently are not consistent. Cox *et al* [2] found magnetic moments larger than the bulk value, but de Heer *et al* found magnetic moments smaller than the bulk value. The ionization potentials (IPs) of iron clusters have also been measured by a few authors [4, 5, 6]. Generally the ionization potentials decrease rapidly but non-monotonically up to  $N \sim 20$ , beyond which the ionization potentials evolve more slowly and smoothly. Unlike for alkali-metal clusters, the results from the liquid droplet model for ionization potentials of iron clusters do not agree well with experimental data [5, 6], especially in clusters of a few atoms. The measured IPs are lower than those predicted by the conducting spherical droplet model. To understand completely the observed magnetic properties of iron cluster and the other physical properties changing from the atom to the bulk phase, it is necessary to study the atomic structures and magnetic properties of small iron clusters.

A few calculations on fragments of bulk iron phases have been performed since the beginning of 1980s [7, 8]. In these studies, the magnetic moments and electronic properties are found to converge to the bulk values very quickly. Actually, in small clusters, most of the atoms are on the surface, the structures of the small clusters can be very different from the fragments of bulk phases, and different structures might have quite different

electronic and magnetic properties. Cheng *et al* [9] made calculations for  $\text{Fe}_2$ ,  $\text{Fe}_3$  and  $\text{Fe}_4$  in ferromagnetic, paramagnetic and antiferromagnetic states by using the linear combination of atomic orbitals method. They found that the lowest-energy state is the ferromagnetic state, and that the equilibrium interatomic distances are much smaller than the nearest-neighbour distance in the bulk phase, while the magnetic moments are larger than that of the bulk phase. The ground-state properties of small iron clusters have also been studied using the effective-medium theory [10], and an observable difference has been found in the bond lengths, binding energies and magnetic moments on comparing with the results obtained by first-principles methods. Some model Hamiltonians [11] have also been used to study the small iron clusters.

In this paper, we report theoretical results for small iron clusters with  $N \leq 7$  obtained using spin-density functional theory with the Barth–Hedin local spin-density approximation (LSDA) [12]. It is known that the gradient correction to the LSDA for the phase diagram of bulk iron is important [13], but in the present studies we find that the energy difference between the different structures is large, so we can assume that the gradient correction to the LSDA will not change the results of the present calculation significantly. The linear combinations of atomic wave functions of 3d, 4s and 4p orbitals have been used as the basis functions. The Kohn–Sham equation is solved by the discrete variational method which has been discussed in detail by Ellis *et al* [14]. The calculations including more diffusive 4d orbitals show very small effects on the binding energy, magnetic moments and equilibrium distances. The frozen-core approximation has been used in all the calculations. The binding energies of the clusters are calculated from  $E_b = E_{\text{ref}} - E_t$ , where  $E_t$  is the total energy of the cluster and  $E_{\text{ref}}$  is the sum of the total energies of free atoms, and the zero-point energy is not included in the binding energy calculation. The equilibrium atomic structures of the clusters are obtained by maximizing the binding energy  $E_b$  with respect to the interatomic distances, within the symmetry constraints. Mulliken population analysis has been used to obtain the occupation number of atomic orbitals, and the magnetic moments are the differences between the occupation numbers in spin-up and spin-down states. The vertical ionization potentials are the total energy differences between neutral and positively charged clusters at the equilibrium distances of the neutral clusters.

**Table 1.** The equilibrium bond length  $R_c$  (Å), vibrational frequency  $\omega_c$  ( $\text{cm}^{-1}$ ), and binding energy  $E_b$  (eV) for the  $\text{Fe}_2$  dimer.

	$R_c$	$\omega_c$	$E_b$ / per atom
Present calculation			
Ferromagnetic	2.09	368	1.65
Antiferromagnetic	2.18	182	0.85
Chen [9]			
Ferromagnetic	1.98	418	2.03
Antiferromagnetic	2.20	209	0.96
Harris and Jones [18]	2.10	390	1.73
Shim and Gingerich [16] <sup>a</sup>	2.46	226	1.10
Shim and Gingerich [16] <sup>b</sup>	2.40	204	1.74
Experimental values [15]	2.02, 1.87	299	

<sup>a</sup> CI Calculation.

<sup>b</sup> HF Calculation.

We have calculated the equilibrium structures of small iron clusters for up to seven atoms. The structural data for the dimer are listed in table 1, where they are compared with

available theoretical and experimental results. Several LSDA calculations on the equilibrium structures of small iron clusters of up to only four atoms have been reported [9, 10], and our equilibrium structures are similar to those found by other authors [9, 10]. We have found the equilibrium bond length to be 2.09 Å for the iron dimer, which is in good agreement with EXAFS studies of matrix-isolated Fe<sub>2</sub> which give an interatomic distance between 1.87 Å and 2.02 Å [15]. This bond length is considerably smaller than the nearest-neighbour distance 2.5 Å of bulk BCC crystalline iron. The binding energy obtained, 1.61 eV, is much larger than the value of ~0.8 eV for the experimental binding energy determined by Knudsen cell mass spectrum matrix measurements [16]. The large difference between the experimental data and the present results for the binding energy might be attributed to the LSDA method. In fact, other calculations also obtained very large binding energies as given in table 1, but the CI calculation got a value closer to the experimental data. The vibrational frequency calculated in the harmonic approximation near the equilibrium bond length is about 368 cm<sup>-1</sup>, as usual in the LSDA, which is also larger than the experimental value of 299 cm<sup>-1</sup> determined by Moskovits and Di Lella [17], because the LSDA always tends to have higher charge density. A small difference of vibrational frequency was also observed between the present work and other calculations, but the CI calculation obtained rather a small vibrational frequency. We have also studied the antiferromagnetic states of Fe<sub>2</sub>, and obtained the equilibrium distance as 2.20 Å, which is about 0.1 Å larger than that in the ferromagnetic state. The binding energy is about 0.8 eV lower, as shown in table 1.

Table 2. The binding energy  $E_b$  (eV), magnetic moment per atom, ionization potentials  $\mathcal{I}$  (eV) and average bond length  $D_0$  (Å) for all calculated small iron clusters.

Cluster	$E_b$ / per atom	$\mu_b$	$\mathcal{I}$	$D_0$
Fe <sub>3</sub>				
Chain	1.812	3.53	6.8	2.13
Triangle	2.036	3.98	5.70	2.37
Fe <sub>4</sub>				
Tetrahedron	2.667	3.01	5.68	2.32
Rhombus	2.606	3.41	5.51	2.36
Square	2.489	3.55	4.99	2.33
Fe <sub>5</sub>				
Rhombus pyramid	3.062	3.31	5.06	2.39
Triangle bipyramid	3.199	3.45	5.18	2.43
Pentagon	2.390	3.35	4.97	2.49
Fe <sub>6</sub>				
Octahedron	3.592	3.30	5.53	2.38
Pentagon pyramid	3.203	3.33	4.95	2.34
Hexagonal	2.477	3.49	5.70	2.33
Fe <sub>7</sub>				
Capped octahedron	3.634	3.14	5.39	2.54
Pentagon bipyramid	3.754	2.85	5.21	2.42
Hexagonal pyramid	3.302	3.39	5.48	2.45

The calculated physical and structural properties of the Fe<sub>3</sub>–Fe<sub>7</sub> cluster are given in table 2. In the case of the Fe<sub>3</sub> cluster, we have calculated the linear and triangle geometric structures. The binding energy of the triangle structure is about 0.67 eV higher than that of the linear structure; this is consistent with the results of other theoretical calculations [9, 10]. We have studied Fe<sub>4</sub> clusters with square, rhombus and tetrahedron structures. We found the

tetrahedron structure to be the structure with the largest binding energy, in agreement with other theoretical studies, which indicates that a transition from a two-dimensional structure to a three-dimensional one takes place at  $N = 4$ . In the larger clusters, we also found the planar structures to have very small binding energy. There is a large difference between the bond lengths for  $\text{Fe}_N$  ( $N = 2, 3, 4$ ) and Chen and Christensen's results; however, the value that we have obtained is in between.

For the cluster  $\text{Fe}_5$ , we found the compact triangle bipyramid structure to have the largest energy, the rhombus pyramid to have energy only slightly lower, but the pentagonal structure for  $\text{Fe}_5$  cluster has very small binding energy. We found the octahedral structure to have the largest binding energy for the  $\text{Fe}_6$  cluster, and the binding energy of the pentagonal pyramid structure to be very close to that of the equilibrium structure, while the planar hexagonal structure has much smaller binding energy. For the  $\text{Fe}_7$  cluster, the energy with the largest binding structure is the pentagonal bipyramid; the capped octahedron has a slightly smaller binding energy.

From table 2, we can see that the binding energies increase quickly as the size increases, but are still far from the theoretical bulk phase value of 5.9 eV [19]. However, we can also see that the average bond distance  $D_0$ , starting at 2.09 Å in the dimer, increases to 2.54 Å which is close to the nearest-neighbour distance in the bulk BCC phase. The ionization potentials and their dependences on cluster size can shed light on the electronic structures of the clusters. In the present study, the ionization potentials are obtained by calculating the binding energy difference between neutral and positively charged clusters at equilibrium distance. From figure 1, we can see that the calculated ionization potentials are in reasonably good agreement with experimental data, except for the shift of about 0.5 eV to lower values. It is also worth noting that the ionization potentials are strongly dependent on the atomic structures (see table 2); for each cluster, different structures have different ionization potentials. Hence to understand the physical properties of the small iron clusters, it is necessary to calculate the true ground-state structure.

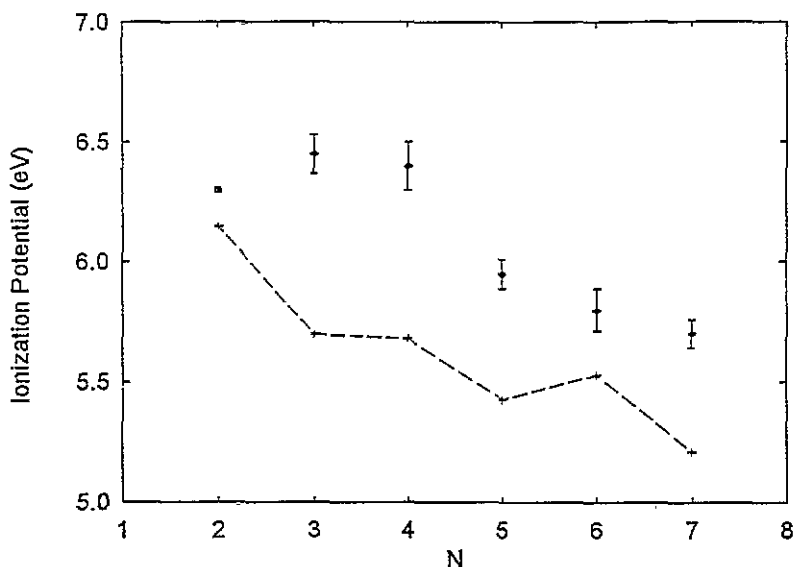


Figure 1. The ionization potentials for small iron clusters. The dots with error bars are experimental results from [4]; the solid line shown the results of the present calculation.

In all the clusters for which we made calculations (up to seven atoms), we find that the

magnetic moments are generally larger than the bulk value ( $2.21\mu_B/\text{atom}$ ) in BCC phase. The total magnetic moments increase as the number of atoms in the cluster increases, but the magnetic moment per atom fluctuates with the size of the cluster, which is in agreement with experimental data. For the iron dimer, we obtain a value of about  $7.6\mu_B$  for the total magnetic moment. A large difference between the values for the neutral and charged dimers has been observed. The magnetic moment for  $\text{Fe}_2^+$  is about  $7.0\mu_B$ . We also obtain a value of about  $11.0\mu_B$  for iron the trimer, and  $9.0\mu_B$  for  $\text{Fe}_3^+$ . As we will show later, most of the electrons near the Fermi level are in the spin-up state, which is why the magnetic moment decreases upon ionization. The magnetic depletion experiments [2] gave  $(6.5\pm 1)\mu_B$  for  $\text{Fe}_2^+$  and  $(8.1\pm 1)\mu_B$  for  $\text{Fe}_3^+$ . We can see that for the charged clusters, a good agreement between the theoretical and experimental data has been reached; but there are no direct experimental data on the magnetic moments for the neutral dimer and trimer to compare with. In all the clusters, we have also obtained a small magnetic moments for sp electrons ( $\sim -0.1\mu_B$ ). In figure 2, the average magnetic moments for neutral and positively charged clusters at the equilibrium bond lengths are shown, and the experimental results of Cox *et al* [2] are also replotted for comparison. We can see that the agreement with experiment is quite good, except that we get a slightly smaller value at the most compact structure, the bipyramid  $\text{Fe}_7$ . We have also tried to calculate the magnetic moments at distances which are a little bit larger than equilibrium distances, and the results show that the magnetic moments are increased. These results may partially explain why the magnetic moments increase as the temperature of the cluster increases.

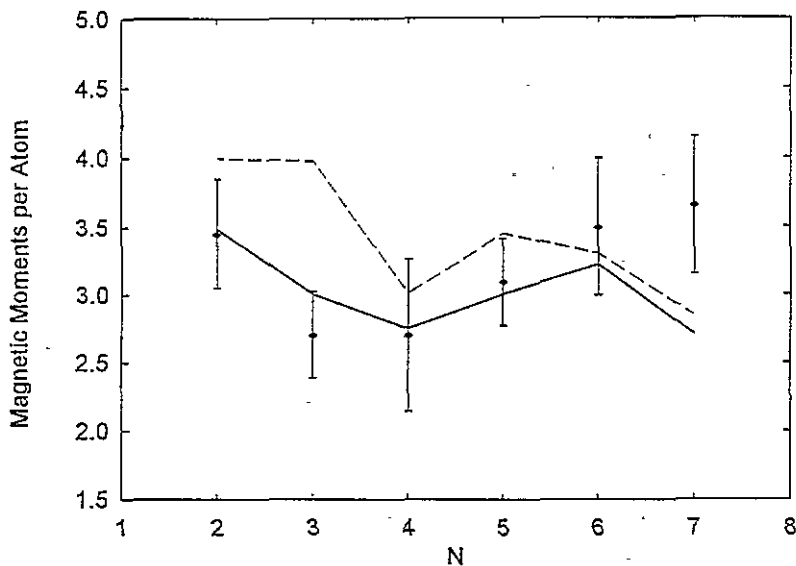


Figure 2. The calculated magnetic moments per atom as a function of cluster size. The dotted line shows the results for neutral clusters, the solid line shows the results for positively charged clusters, and the dots with error bars are the experimental results from [2].

Since, in the clusters, the thermal expansion coefficients can be very large, when the temperature increases, the cluster expands, which can lead to a larger magnetic moment. For each cluster, the more compact the structure is, the smaller the magnetic moment. This is not surprising because in the small clusters, the atoms have fewer neighbours than in the bulk, and therefore the kinetic energy will not increase much upon magnetization. Hence the magnetic moment in the cluster will have a larger value than that in the bulk. The number of

nearest neighbours in the compact structure is larger than that in the loose structures; it will 'cost' more energy to have large magnetism, so the compact structures tend to have smaller magnetic moments. This phenomenon has also been already observed in the surface.

**Table 3.** The average Mulliken populations for small iron clusters at the bond length with the largest binding energy, magnetic moments per atom and exchange splitting  $\Delta E_{xc}$ . The numbers in brackets are for positively charged clusters.

Cluster	3d	4s	4p	$\mu$	$\Delta E_{xc}(d)$	$\Delta E_{xc}(sp)$
2	6.395 (6.443)	1.300 (0.940)	0.305 (0.116)	4.00 (3.49)	2.4-3.0	1.0-2.0
3	6.389 (6.554)	1.202 (0.859)	0.409 (0.253)	3.98 (3.00)	2.3-3.0	0.9-1.9
4	6.513 (6.583)	0.998 (0.838)	0.489 (0.330)	3.00 (2.75)	1.9-2.5	0.7-1.4
5	6.423 (6.527)	1.095 (0.907)	0.482 (0.366)	3.45 (3.00)	2.0-2.7	0.8-1.7
6	6.482 (6.523)	1.000 (0.942)	0.518 (0.368)	3.30 (3.22)	2.0-2.4	0.9-1.6
7	6.509 (6.535)	0.929 (0.901)	0.567 (0.422)	2.85 (2.71)	1.3-2.5	0.5-1.2

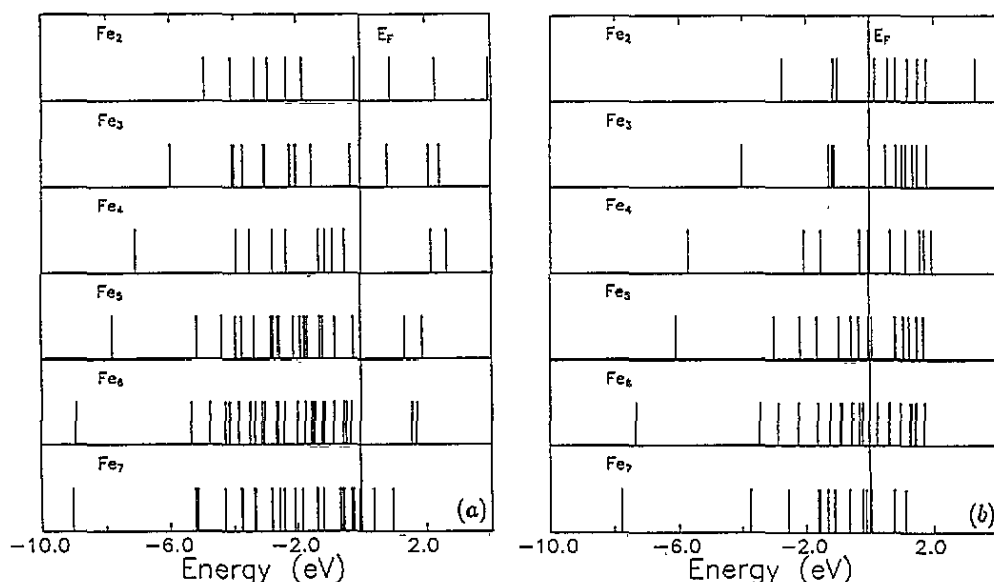


**Figure 3.** The eigenvalue spectrum for the small iron clusters: (a) for spin-up states; (b) for spin-down states.

In table 3, the average 3d, 4s, 4p Mulliken populations for neutral and positively charged clusters for the structure with the largest binding energy have been given. As the size of cluster increases from Fe<sub>2</sub> to Fe<sub>7</sub> clusters, the average number of d electrons and of the 4p electrons increase by up to about 0.5 electron, which indicates the increasing sp-d hybridization. We can also see that the ionized electrons are seen to come largely from 4s and 4p orbitals. Comparing to that for neutral clusters, the number of s electrons also

increases, and this might be why the magnetic moments decrease upon ionization.

The eigenvalue distributions for all the clusters calculated are shown in figure 3, with the Fermi energy shifted to zero in all the cases. We can see that the band width increases gradually from the Fe<sub>2</sub> to the Fe<sub>7</sub> cluster. For Fe<sub>2</sub> dimers, the total occupied band width is about 5 eV. For the Fe<sub>7</sub> cluster, the total occupied band width is about 9 eV, which is already close to the theoretical bulk band width [19]. For the spin-down states, the total occupied band width is about 1–2 eV narrower than that of spin-up states. The exchange splitting differs from cluster to cluster, and the values are listed in table 3. Although as the size of cluster increases the exchange splitting decreases, the exchange splitting in Fe<sub>7</sub> is still larger than the bulk value of about 1.1–2.2 eV for d states and about 0.16–0.85 eV for sp states. These values are consistent with other LSDA work [7] which found  $\approx 1.8$ –3.2 eV for the d states in the Fe<sub>9</sub> cluster and  $\approx 1.0$ –2.7 eV for the d states in Fe<sub>15</sub> clusters. Comparing to the eigenvalues in the spin-up and spin-down states, we can find that the electrons near the Fermi level are largely from the spin-up states, so the ionization, which reduced the number of electrons in the spin-up states, will decrease the magnetic moments.

In summary, we have performed LSDA calculations for the small iron clusters. The equilibrium state structures are obtained through binding energy calculations. We found that the small iron clusters tend to have a compact structure. Beginning at  $N = 4$ , the binding energies of planar structures are very small. The calculated ionization potentials are in good agreement with experimental data. The magnetic moments are found to be larger than the bulk values. With the increase of cluster size, generally the magnetic moment per atom decreases. These results are in agreement with experimental data of Cox *et al* [2]. We have also observed a small charge transfer between the sp and d states because of the sp–d hybridization. For the Fe<sub>7</sub> cluster, we found that the occupied band width and the average equilibrium distance are close to the bulk-phase values, but that other physical properties, like the magnetic moments and ionization potentials, are far from the bulk values.

## Acknowledgment

This work was supported by the Climbing Research Program-National Fundamental Project.

## References

- [1] Berkowitz A E 1992 *Magnetic Properties of Fine Particles* ed J L Dormann and D Fiorani (Amsterdam: North-Holland)
- [2] Cox D M, Trevor D J, Whetten R L, Rohlfing E A and Kaldor A 1985 *Phys. Rev. B* **32** 7290
- [3] de Heer W A, Milani P and Chatelain A 1990 *Phys. Rev. Lett.* **65** 488; 1991 *Z. Phys. D* **19** 241
- [4] Rohlfing E A, Cox D M, Kaldor A and Johnson K H 1984 *J. Chem. Phys.* **81** 3846
- [5] Yang Shihe and Knickelbein M B 1990 *J. Chem. Phys.* **93** 1533
- [6] Parks E K, Kplots T D and Riley S J 1990 *J. Chem. Phys.* **92** 3813
- [7] Yang C Y Y, Johnson K H, Salahub D R and Kaspar J 1981 *Phys. Rev. B* **24** 5673
- [8] Salahub D R and Messmer R P 1981 *Surf. Sci.* **106** 415
- [9] Chen J L, Wang C S, Jackson K A and Pederson M R 1991 *Phys. Rev. B* **44** 6523
- [10] Christensen O B and Cohen M L 1993 *Phys. Rev. B* **47** 13643
- [11] Pastor G M, Dorantes-Davila J and Bennemann K H, 1989 *Phys. Rev. B* **40** 7642  
Dorantes-Davila J, Dreyse H and Pastor G M 1992 *Phys. Rev. B* **46** 10432
- [12] Barth U and von Hedin L 1972 *J. Phys. C: Solid State Phys.* **5** 1629
- [13] Amador C, Lambrecht W R L and Segall B 1992 *Phys. Rev. B* **46** 1870
- [14] Ellis D E and Painter G S 1970 *Phys. Rev. B* **2** 2887  
Delley B and Ellis D E 1982 *J. Chem. Phys.* **76** 1949
- [15] Purdum H, Montano P A, Shenoy G K and Morrison T 1982 *Phys. Rev. B* **25** 4412
- [16] Shim I and Gingerich K A 1982 *J. Chem. Phys.* **77** 2490



- [17] Moskovits M and Di Lella D P 1980 *J. Chem. Phys.* **73** 4917
- [18] Harris J and Jones R O 1979 *J. Chem. Phys.* **70** 830
- [19] Moruzzi V L, Janak J F and Williams A R 1978 *Calculated Electronic Properties of Metals* (Oxford: Pergamon)